

SMOTE and Mirrors: Exposing Privacy Leakage from Synthetic Minority Oversampling*

Georgi Ganev^{1,2}, Reza Nazari¹, Rees Davison¹, Amir Dizche¹, Xinmin Wu¹,
Ralph Abbey¹, Jorge Silva¹, Emiliano De Cristofaro³

¹SAS ²UCL ³UC Riverside

georgi.ganev@sas.com

Abstract

The Synthetic Minority Over-sampling Technique (SMOTE) is one of the most widely used methods for addressing class imbalance and generating synthetic data. Despite its popularity, little attention has been paid to its privacy implications; yet, it is used in the wild in many privacy-sensitive applications. In this work, we conduct the first systematic study of privacy leakage in SMOTE: We begin by showing that prevailing evaluation practices, i.e., naive distinguishing and distance-to-closest-record metrics, completely fail to detect any leakage and that membership inference attacks (MIAs) can be instantiated with high accuracy. Then, by exploiting SMOTE’s geometric properties, we build two novel attacks with very limited assumptions: *DistinSMOTE*, which perfectly distinguishes real from synthetic records in augmented datasets, and *ReconSMOTE*, which reconstructs real minority records from synthetic datasets with perfect precision and recall approaching one under realistic imbalance ratios. We also provide theoretical guarantees for both attacks. Experiments on eight standard imbalanced datasets confirm the practicality and effectiveness of these attacks. Overall, our work reveals that SMOTE is inherently non-private and disproportionately exposes minority records, highlighting the need to reconsider its use in privacy-sensitive applications.

1 Introduction

From rare disease diagnosis to fraud detection, machine learning tasks can be profoundly affected by severe class imbalance, where instances of interest – the minority class – are much rarer than the majority class [26]. Models often underperform under these conditions, exhibiting biases toward the majority and failing to capture the minority reliably [9]. One of the most influential and widely adopted approaches to address this is the Synthetic Minority Over-sampling Technique (SMOTE) [7], which augments the imbalanced data by upsampling or generating synthetic samples of the underrepresented class through linear interpolation between minority records. Due to its simplicity and effectiveness, SMOTE continues to play a central role in real-world applications. To put things in context, the SMOTE paper has been cited nearly 40k times, Microsoft Azure offers built-in SMOTE components [40, 41], and most MLaaS services support it [5, 23]. Overall, SMOTE is primarily used in two contexts: 1) as a data augmentation technique for machine learning classifiers, and 2) as a synthetic data generation method to facilitate data sharing.

Data Augmentation. SMOTE was originally proposed as a pre-processing/upsampling technique to augment the real dataset, thus improving classifier performance, especially F1 score and recall, when trained on the augmented data. Practitioners rely on SMOTE in a wide range of medical applications, including cancer diagnosis [18], heart-related diseases [17, 43], diabetes prediction [2, 51], genetic risk prediction [33], etc. Beyond medicine, SMOTE is widely applied in finance, particularly for credit-card fraud detection [31, 60] and predicting customer churn [46, 49].

*To appear in the 14th International Conference on Learning Representations (ICLR 2026). Please cite the ICLR version.

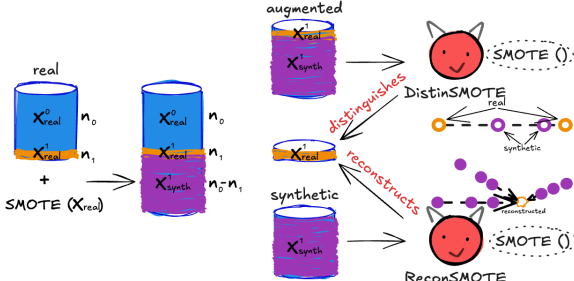


Figure 1: DistinSMOTE and ReconSMOTE attacks vs. augmented/synthetic data generated by SMOTE.

Augmented Data		
Naive	MIA	DistinSMOTE
0.01 ± 0.01	0.68 ± 0.07	1.00 ± 0.00
Synthetic Data		
Naive	MIA	ReconSMOTE
0.16 ± 0.10	0.93 ± 0.02	1.00 ± 0.00

Table 1: Performance of privacy attacks vs. SMOTE. Naive refers to the current privacy evaluation practices. MIAs are applied to SMOTE for the first time. DistinSMOTE and ReconSMOTE are our novel attacks.

Synthetic Data. SMOTE has also gained traction as a method for generating synthetic tabular data. Often used as a benchmark for more advanced models like GANs and VAE, SMOTE has been shown to perform on par with, or even better than, generative approaches [32, 39]. Moreover, it is being used as a reference point for diffusion-based models published at top-tier machine learning conferences [34, 42, 47, 59]. SMOTE remains one of the most widely applied algorithms for medical synthetic data [30], and beyond machine learning research, it has also been recognized as a promising technique for improving access to census data by public sector entities [1, 45].

Roadmap. Although not originally designed with privacy in mind, SMOTE is extensively used in sensitive public-facing applications that process personal data. However, its privacy risks have often been overlooked or significantly underestimated. In this paper, we fill this gap by studying whether, why, and how much privacy leakage occurs from using SMOTE either as a data augmentation method or as a standalone synthetic data generator.

We begin by showing that SMOTE appears to have no privacy leakage when evaluating it through the current practice of training a classifier to distinguish real from synthetic records in augmentation settings or that of measuring the distance from synthetic to real records (more precisely, the distance to closest record, or DCR [61]). We refer to the former as naive distinguishing and the latter as naive metrics. We also instantiate—to our knowledge, for the first time—a Membership Inference Attack (MIA) [53, 56] against SMOTE, showing that attackers can accurately infer whether a target record was part of the real training data.

Next, we propose two *novel* near-perfect privacy attacks with minimal and realistic assumptions: a Distinguishing (DistinSMOTE) and a Reconstruction attack (ReconSMOTE). Both only assume access to a single augmented or synthetic dataset and knowledge that SMOTE generated it (see Figure 1). By exploiting SMOTE’s geometric properties, DistinSMOTE distinguishes real from synthetic records in augmentation settings, while the more ambitious ReconSMOTE reconstructs real minority records from synthetic data. We also provide a theoretical analysis for both attacks, showing they run at worst in $\mathcal{O}(n^2d + n(kr)^2)$, where n , d , and k denote, respectively, the number of input records, features, and SMOTE neighbors, and r represents the data imbalance ratio. While quadratic in n , the complexity remains practical (especially with optimized search), with both attacks running within minutes on all datasets we experiment with.

DistinSMOTE achieves perfect precision and recall, while ReconSMOTE reaches perfect precision—which is more critical in privacy attacks [6]—with recall increasing exponentially (with rate $\approx r/k$), reaching 1 under realistic parameter values ($k = 5$, $r \geq 20$).

Our experiments on eight standard imbalanced datasets, summarized in Table 1, demonstrate that:

- Naive distinguish (0.01 precision)/metrics (0.16 accuracy) completely underestimate risks.
- State-of-the-art MIAs achieve 0.68 AUC on augmented and 0.93 on synthetic data for 100 vulnerable targets, although being time-consuming. Also, sensitivity of targets increases when classifiers are trained on augmented vs. real data, yielding a 17% rise in MIA AUC.
- DistinSMOTE perfectly detects the real records in an augmented dataset.
- ReconSMOTE achieves perfect precision when reconstructing real minority records from a single synthetic

dataset. While its average recall is 0.85, it reaches 1 for imbalance ratios of 20 or higher, consistent with our theoretical analysis.

Implications. Our findings provide further evidence that privacy cannot be treated as an afterthought when applying non-private techniques like SMOTE in sensitive settings. Its use not only risks exposing individual records but can also undermine trust in data-driven systems that rely on synthetic data. Overall, our work has the following real-world implications for researchers/practitioners:

1. SMOTE is fundamentally non-private: its interpolation process makes privacy leakage inherent, not a matter of flawed implementation.
2. Minority records are disproportionately at risk: the very samples SMOTE aims to amplify and make more representative are also the most exposed.
3. Caution is critical: performance gains from oversampling must be weighed vs. privacy risks.

2 Preliminaries

Notation. Let $D_{real} = (X, y)$ be a training dataset, where $X \subseteq \mathbb{R}^{n \times d}$ is the feature matrix consisting of n samples with d -dimensional feature vectors and $y \in \{0, 1\}^n$ the corresponding binary labels. The dataset consists of n_0 majority and n_1 minority records, with imbalance ratio $r = \frac{n_0}{n_1} > 1$. In practice, $n_0 \gg n_1$, which makes learning directly from the minority class challenging.

SMOTE [7] addresses class imbalance by generating synthetic minority samples; see Algorithm 1. To create a synthetic record, a random minority record from D_{real} is selected, one of its k nearest minority neighbors is chosen, and a new point is generated by interpolating along the line segment between them. Repeating this process yields D_{syn} with $n_0 - n_1$ new samples, balancing the class distribution. The synthetic data can be used as a standalone synthetic dataset (D_{syn}) or to form an augmented dataset $D_{aug} = D_{real} \cup D_{syn}$, e.g., to improve classification performance.

Privacy Attacks. Membership Inference Attacks (MIAs) [53, 56] and Reconstruction Attacks [3, 13] are standard tools to empirically measure privacy leakage in ML. In MIAs, the adversary aims to infer whether a target record (x_T, y_T) was part of the training dataset D_{real} . The attack can be framed as a repeated binary classification game: the adversary is given either a classifier (or a synthetic dataset) trained on D_{real} , or one trained on the neighboring $D'_{real} = D_{real} \setminus (x_T, y_T)$, and infers which dataset was used. To do so, the adversary typically exploits differences in model behavior – such as prediction confidences on the target, or statistical features extracted from synthetic data.

In a reconstruction attack, the adversary aims to recover any full real records (i.e., an untargeted attack) from access to a released model or synthetic data. These attacks often assume access to auxiliary information, such as public data, accurate statistics, or limited query access to D_{real} .

We also consider distinguishing attacks, which are somewhat related to MIAs but focus on whether a record comes from the population-level data distribution rather than from the specific dataset used to train the model. In the context of SMOTE, we use these attacks to distinguish unlabelled records in D_{aug} as either real (D_{real}) or synthetic (D_{syn}), since $D_{real} \cap D_{syn} = \emptyset$.

3 Related Work

As discussed in Section 1, SMOTE is widely used for data augmentation and synthetic data generation across various domains. Despite its popularity, prior work has focused primarily on its utility, while its privacy risks remain largely unexplored.

SMOTE has recently served as a baseline in several diffusion-based generative models [34, 42, 47, 59], all published at top-tier machine learning venues. These studies primarily rely on the Distance to Closest Record (DCR) [61] as a privacy proxy, consistently showing smaller distances for SMOTE and claiming this as evidence of weaker privacy. Kotelnikov et al. [34] additionally employ the “full black-box” attack from [8], which still reduces to DCR as its core signal.

More recently, this view has been challenged by Sidorenko and Tiwald [54], who show that some diffusion models [34, 42] achieve lower DCR values than SMOTE, thereby leaking more information about the training data. However, DCR itself has been shown to be an inadequate privacy metric, which consistently underestimates privacy leakage [4, 19, 28, 57]. To the best of our knowledge, SMOTE has not yet been systematically evaluated with state-of-the-art MIAs or through reconstruction attacks, leaving a critical gap in understanding its privacy risks.

4 Privacy Attacks vs. SMOTE

In this section, we present our two novel privacy attacks that expose privacy leakage from SMOTE.

4.1 Adversarial Model

Assumptions. For both attacks, we assume an adversary with access to a *single* dataset generated by SMOTE (D_{aug} for DistinSMOTE and D_{syn} for ReconSMOTE). The adversary knows that the original SMOTE algorithm [7] was applied (Algorithm 1) and is aware of its parameters, specifically, the number of neighbors k and the real data imbalance ratio r (in practice, these can be approximated from the released dataset). The adversary relies solely on the geometrical properties of SMOTE to achieve its goals – either distinguishing or reconstruction. Unlike prior privacy attacks, no further knowledge is required: e.g., the adversary does not need access to public/representative data, repeated inference or generation, the model parameters, numerous shadow models or a meta-classifier (as in MIAs [4, 28, 56]), or published (accurate) aggregate statistics (as in reconstruction [11, 13]).

Objectives. For DistinSMOTE, the adversary aims to distinguish the real minority records from synthetic ones from observing D_{aug} , whereas for ReconSMOTE, to reconstruct them from D_{syn} . We focus on minority records from underrepresented regions of the feature space because they often correspond to the most vulnerable individuals. Such records carry the greatest privacy risks: they are easier to single out, more likely to be re-identified, and any disclosure disproportionately affects the individuals they represent [35, 56]. Indeed, regulators, including the UK Information Commissioner’s Office [29], have explicitly stressed the need to protect minority and outlier records.

We measure the attacks success using precision (the fraction of identified records that are truly real) and recall (the fraction of successfully identified real records), two standard metrics that together give a comprehensive view of performance. In privacy attacks, precision is especially critical, since even a handful of correctly identified records with high confidence can constitute a serious breach [6]. While secondary, capturing a large fraction of minority records is also important.

Data Assumptions. Our theoretical analysis of DistinSMOTE and ReconSMOTE relies on the following three realistic assumptions about the feature structure of the real minority records (X_{real}^1) and k :

Assumption 1 (Real-valued features). *All features in X_{real}^1 are real-valued.*

Assumption 2 (Global non-collinearity). *No three distinct feature vectors in X_{real}^1 are collinear.*

Assumption 3 (Minimum k). *The number of neighbors, $k \geq 3$.*

In other words, all features are continuous and no three points lie on the same line. These assumptions are reasonable for (high-dimensional) continuous data and hold for all datasets in our experiments (see Section 5). Moreover, assuming $k \geq 3$ is necessary to uniquely identify the intersection point of the lines formed by vectors connecting neighboring points, and is a reasonable choice in practice.

4.2 Distinguishing Attack

In Algorithm 2, we outline the DistinSMOTE attack, which distinguishes *real* minority records from synthetic ones within an augmented dataset. The attack exploits the fact that, among any three collinear points, the middle one must be synthetic, since real points are non-collinear and SMOTE generates points strictly between them. The algorithm begins by searching from the convex hull of the minority records and iteratively explores neighbors inwards. When a collinear triplet is found, its midpoint is pruned from the candidate set with real points, and its neighbors are added to the queue for further inspection.

Complexity. The nearest-neighbor search is the main cost. With brute-force search ($\mathcal{O}(nd)$ per query), each of the n records requires finding kr neighbors ($\mathcal{O}(nd)$) and checking all neighbor pairs ($\mathcal{O}((kr)^2)$), yielding a worst-case complexity of $\mathcal{O}(n^2d + n(kr)^2)$. In practice, optimized methods (e.g., KD/ball trees) reduce search to $\mathcal{O}(\log n)$ for small d ($d \leq 32$ in our datasets). Also, since k and r are typically (small) constants, the effective complexity is much lower, and the algorithm completes in under three minutes on all tested datasets.

Accuracy Analysis. We now analyze the expected performance of DistinSMOTE.

Theorem 1 (DistinSMOTE perfect precision & recall). *Under Assumptions 1–2, the labeling rule proposed by the DistinSMOTE attack achieves perfect precision and recall.*
Proof. By SMOTE construction, each synthetic point lies strictly on the line segment between two real points ($x_{syn} = x_i + u(x_j - x_i)$). Under the global non-collinearity assumption, no three real points are collinear, so any line in D_{aug} containing at least three points consists of exactly two real endpoints $x_i, x_j \in X_{real}^1$ and one or more synthetic interior points $x_{m_1}, x_{m_2}, \dots \in X_{syn}^1$.

DistinSMOTE follows this labeling rule: for such lines, it marks interior points as synthetic and endpoints as real, while any real point not on such a line (i.e., not used in interpolation) is also labeled real. This ensures all synthetic points are eliminated and all real points are preserved. This leads to perfect precision and recall (“real” is the positive class). \square

4.3 Reconstruction Attack

Algorithm 3 presents the ReconSMOTE attack, which operates solely on synthetic data. The attack relies on two main intuitions: 1) synthetic records lie along line segments connecting real minority points, so these lines can be detected by finding three or more collinear samples, and 2) such lines intersect exactly at the original real points. The algorithm begins by iteratively defining lines, searching each point and two of its neighbors for collinear triplets, and then extending them with additional collinear neighbors. For each line, the mean of its points is stored as a midpoint, providing a compact representation of the line’s location. Next, the algorithm examines pairs of midpoints to identify intersection points of the corresponding lines, which serve as candidate real records. Finally, we retain only intersections supported by at least three distinct lines, filtering out spurious candidates.

Complexity. The worst-case time complexity is very similar to DistinSMOTE, i.e., $\mathcal{O}(n^2d + n(kr)^2)$. While there are two additional factors, namely, $\mathcal{O}(nkr)$ for checking neighbors after identifying a collinear triplet and $\mathcal{O}(n^2)$ for finding line intersections, these are dominated by existing terms and can be ignored. The practical complexity is much lower, and the attack runs in at most three minutes on all datasets.

Accuracy. Next, we analyze ReconSMOTE’s expected performance.

Algorithm 2 DistinSMOTE

```

Require: Augmented data  $D_{aug}$ 
Require: Number of neighbors  $k$ , imbalance ratio  $r$ 
Ensure: Detected real minority records  $C^1$ 
1 Filter minority  $X_{aug}^1 \leftarrow \{X_{aug}[i] | y_{aug}[i] = 1\}$ 
2 Initialize candidate set  $C^1 \leftarrow X_{aug}^1$ 
3 Initialize queue  $queue \leftarrow H(X_{aug}^1)$   $\triangleright$  convex hull
4 Initialize visited set  $V \leftarrow \emptyset$ 
5 while  $queue \neq \emptyset$  do
6   for record  $x_i \in queue$  do
7     if  $x_i \notin V$  and  $x_i \in C^1$  then
8       Add  $x_i$  to  $V$ 
9       Find  $2 \cdot k \cdot r$  nearest neighbors of  $x_i$ ,  $N(x_i)$ 
10      for pairs of neighbors  $(x_j, x_k) \in N(x_i)$  do
11        if  $x_i, x_j, x_k$  are collinear then
12          Identify middle point  $x_m \in \{x_i, x_j, x_k\}$ 
13          Remove  $x_m$  from  $C^1$ ; Add  $x_m$  to  $V$ 
14          Add  $N(x_m) \cap C^1$  to  $queue$ 
15        end if
16      end for
17    end if
18  end for
19 end while
20 return  $C^1$ 

```

Theorem 2 (ReconSMOTE perfect precision). *Under Assumptions 1–3, the records reconstructed by ReconSMOTE are guaranteed to be real, i.e., the attack achieves perfect precision.*

Proof. By SMOTE construction, each synthetic point lies on a segment strictly between two real endpoints. Thus, every detected line in X_{syn}^1 corresponds uniquely to a pair of real records.

Under the global non-collinearity assumption, the only point lying on three or more such lines is the shared real endpoint. Since ReconSMOTE retains only intersections supported by at least three distinct lines (as $k \geq 3$), every reconstructed point must be a true real point. Hence, precision is 1. \square

Theorem 3 (ReconSMOTE expected recall (approximate)). *Let $\lambda = \frac{n_0 - n_1}{n_1 k}$. Under Assumptions 1–3 and using Poisson approximation (treating the number of synthetic points per segment as Poisson), the expected recall of ReconSMOTE satisfies:*

$$\mathbb{E}[\text{Recall}] \geq \max \left\{ 0, \frac{k \left(1 - e^{-\lambda} \left(1 + \lambda + \frac{\lambda^2}{2} \right) \right) - 2}{k - 2} \right\}. \quad (1)$$

Proof. At each generation step, SMOTE first selects a minority record x_i uniformly from the n_1 available, and then one of its k nearest neighbors x_j uniformly. Thus, each of the $n_1 k$ possible minority-neighbor (directed) segments is chosen with probability $\frac{1}{n_1 k}$ at every step.

Let C_{ij} denote the number of synthetic points generated on segment (x_i, x_j) . Since each of the $n_0 - n_1$ synthetic points is assigned independently to a segment with probability $\frac{1}{n_1 k}$, we have $C_{ij} \sim \text{Binom}(n_0 - n_1, \frac{1}{n_1 k})$. For analytic tractability, we approximate this by $\text{Poisson}(\lambda)$ with mean $\lambda = \frac{n_0 - n_1}{n_1 k}$. This is standard when $n_0 - n_1$ is large and $\frac{1}{n_1 k}$ is small, which holds in practice.

A segment is reconstructed if $C_{ij} \geq 3$. The probability of this is $p_{\text{edge}} = \Pr\{\text{Poisson}(\lambda) \geq 3\} = 1 - e^{-\lambda} \left(1 + \lambda + \frac{\lambda^2}{2} \right)$. Now consider a fixed record x_i , and let S_i denote the number of reconstructed segments incident to it. Therefore, $\mathbb{E}[S_i] = k p_{\text{edge}}$. Moreover, by Assumption 3, once $S_i \geq 3$, the point x_i is uniquely identifiable, since three non-collinear reconstructed segments suffice to triangulate its location. To lower bound $\Pr\{S_i \geq 3\}$, observe that $\mathbb{E}[S_i] = \mathbb{E}[S_i \mathbb{I}\{S_i \leq 2\}] + \mathbb{E}[S_i \mathbb{I}\{S_i \geq 3\}] \leq 2 \Pr\{S_i \leq 2\} + k \Pr\{S_i \geq 3\}$ (since $S_i \leq k$). As $\Pr\{S_i \leq 2\} = 1 - \Pr\{S_i \geq 3\}$, this yields $\mathbb{E}[S_i] \leq 2 + (k - 2) \Pr\{S_i \geq 3\}$, hence $\Pr\{S_i \geq 3\} \geq \frac{\mathbb{E}[S_i] - 2}{k - 2} = \frac{k p_{\text{edge}} - 2}{k - 2} := A_{id}$.

This is the probability that x_i is identifiable. Since recall is the fraction of minority records that are identifiable, its expectation equals the average of these probabilities over all n_1 records. Because each x_i is treated symmetrically in SMOTE and we look at directed segments, the average equals the bound derived above. Hence we obtain the stated lower bound on the expected recall. \square

Remarks. By rearranging Equation 1, we get $1 - \mathbb{E}[\text{Recall}] \leq \frac{k}{k-2} e^{-\lambda} \left(1 + \lambda + \frac{\lambda^2}{2} \right)$, which in turn means $\mathbb{E}[\text{Recall}] \rightarrow 1$ as $\lambda \rightarrow \infty$, with a convergence rate exponential in $\lambda (= \frac{n_0 - n_1}{n_1 k} = \frac{r-1}{k})$.

For brevity and clarity, Theorem 3 is derived under the Poisson approximation with C_{ij} counted only in one direction. We refer to this as the *approximate* bound. In Appendix A, we provide a more detailed analysis

Algorithm 3 ReconSMOTE

```

Require: Synthetic data  $D_{syn}$ 
Require: Number of neighbors  $k$ , imbalance ratio  $r$ 
Ensure: Reconstructed real minority records  $R^1$ 
1 Filter minority  $X_{syn}^1 \leftarrow \{X_{syn}[i] | y_{syn}[i] = 1\}$ 
2 Initialize reconstructed set  $R^1 \leftarrow \emptyset$  and
   line support map  $S \leftarrow \emptyset$ 
3 Initialize set of lines  $\mathcal{L} \leftarrow \emptyset$ , midpoints  $\mathcal{M} \leftarrow \emptyset$ 
4 Initialize visited set  $V \leftarrow \emptyset$ 
5 for record  $x_i \in X_{syn}^1$  do
6   if  $x_i \notin V$  then
7     Add  $x_i$  to  $V$ 
8     Find  $2 \cdot k \cdot r$  nearest neighbors of  $x_i$ ,  $N(x_i)$ 
9     for pairs of neighbors  $(x_j, x_k) \in N(x_i)$  do
10       if  $x_i, x_j, x_k$  are collinear then
11         Form initial line  $(x_i, x_j, x_k)$ ; Add  $x_j, x_k$  to  $V$ 
12         for neighbor  $x_n \in N(x_i) \setminus \{x_i, x_j, x_k\}$  do
13           if  $x_n$  collinear with line  $(x_i, x_j, x_k)$  then
14             Add  $x_n$  to line  $(x_i, x_j, x_k)$ ; Add  $x_n$  to  $V$ 
15           end if
16         end for
17         Add line to  $\mathcal{L}$ 
18         Compute mean of line points and add to  $\mathcal{M}$ 
19       end if
20     end for
21   end if
22 end for
23 for pairs of midpoints  $(m_p, m_q) \in \mathcal{M}$  do
24   Compute intersection point  $x^*$  of lines
   corresponding to  $m_p$  and  $m_q$ 
25   Add  $x^*$  to  $R^1$  and record support line
   indices  $\{p, q\}$  in  $S(x^*)$ 
26 end for
27 Filter points in  $R^1$  with  $|S(x^*)| \geq 3$ 
28 return  $R^1$ 

```

and derive a tighter bound without these simplifications; we call it the *exact* bound. Finally, in Appendix B, we visualize the differences between the bounds under various conditions.

5 Experimental Evaluation

We now evaluate the effectiveness of our novel attacks, along with additional methods geared to assess privacy leakage in SMOTE, both as a data augmentation and synthetic data generation technique. Specifically, we consider: 1) current practices such as naive distinguish (via a classifier) and privacy metrics (i.e., DCR from synthetic to real records [61]), 2) state-of-the-art Membership Inference Attacks (MIAs) [6, 53], which to the best of our knowledge have not yet been applied against SMOTE, and 3) the DistinSMOTE and ReconSMOTE attacks. Overall results are summarized in Table 1.

Datasets. We conduct experiments on eight standard imbalanced datasets, each with a binary classification task, obtained from the imblearn library [37] (originally from the UCI ML Repository) and used in prior work [12, 52]. These datasets vary quite significantly in size (336 to 11,183 records), dimensionality (6 to 32 features), imbalance ratios (8.6 to 130), and prediction task (target), as shown in Table 2.

Implementations. We use the imblearn [37] implementation of SMOTE and sklearn [48] for machine learning classifiers. Both DistinSMOTE and ReconSMOTE are highly efficient, running in under three minutes on any dataset on an Apple M4 MacBook with 24GB RAM. The naive methods are similarly fast, while the MIAs require up to 30 minutes per dataset. We will release the source code for our attacks along the final version of the paper.

5.1 Augmented Data

We compare the three approaches on augmented data, with results for all datasets shown in Table 3.

Naive Distinguish is a popular but arguably misguided approach for telling apart real and synthetic records by training a classifier [10, 16, 50, 55]. Half of the real and half of the synthetic data are used to train a Random Forest classifier, with testing performed on the remaining data. For each dataset, we run 5 independent SMOTE generations and train 5 classifiers per run, reporting averaged results. The method severely underestimates privacy risk (see the two leftmost columns in Table 3; precision and recall ≈ 0) as it is capable of capturing only distributional differences, not record-level leakage.

Membership Inference. Next, we evaluate MIAs [6, 53] using the repeated classification game from Section 2. For a given target record, we train 200 classifiers (a multi-layer perceptron with two hidden layers) on augmented datasets generated via SMOTE: half of the training datasets include the target record, and half exclude it. We then use the classifiers' predictions on the target to simulate an adversary's confidence in distinguishing membership, and calculate AUC. Following prior work [24, 58], we train target-specific attacks in a leave-one-out setting, which provides a more accurate estimate of privacy leakage. This procedure is repeated for 100 randomly selected targets (or all minority records), and we report the average. Overall, this requires training roughly 20k SMOTE models and classifiers per dataset.

Looking at Table 3 (fourth column), the average AUC is 0.68, with half of the datasets exceeding 0.7, which indicates substantial privacy leakage. The lowest scores appear in datasets with the smallest imbalance (ecoli and abalone), where the proportion of synthetic data is relatively low. Mammography also shows a low score, likely because its large number of records reduces the influence of any single individual. These results are therefore not entirely surprising.

We also conduct an additional MIA experiment, training classifiers solely on the real data, to test the intuition that SMOTE enhances the sensitivity of minority records in the augmented data, as they directly contribute to generating synthetic samples. As expected, targets become more vulnerable when augmentation is applied –

Dataset	Target	r	n	d
ecoli	imU	8.6	336	7
abalone	7	9.7	4,177	10
car_eval_34	vgood	12	1,728	21
solarflare_m0	M-0	19	1,389	32
car_eval_4	vgood	26	1,728	21
yeast_me2	ME2	28	1,484	8
mammography	minority	42	11,183	6
abalone_19	19	130	4,177	10

Table 2: Datasets overview, where r denotes the imbalance ratio (n_0/n_1), n the number of records, and d the number of features.

The MIAs require up to 30 minutes per dataset.

Dataset	r	Naive distinguish		MIA		DistinSMOTE	
		D_{aug} (Precision)	D_{aug} (Recall)	D_{real} (AUC)	D_{aug} (AUC)	D_{aug} (Precision)	D_{aug} (Recall)
ecoli	8.6	0.00 ± 0.00	0.00 ± 0.00	0.50 ± 0.04	0.50 ± 0.05	1.00 ± 0.00	1.00 ± 0.00
abalone	9.7	0.03 ± 0.03	0.00 ± 0.01	0.57 ± 0.03	0.58 ± 0.04	1.00 ± 0.00	1.00 ± 0.00
car_eval_34	12	0.01 ± 0.02	0.01 ± 0.01	0.60 ± 0.03	0.73 ± 0.08	1.00 ± 0.00	1.00 ± 0.00
solarflare_m0	19	0.01 ± 0.03	0.00 ± 0.01	0.79 ± 0.03	0.97 ± 0.03	1.00 ± 0.00	1.00 ± 0.00
car_eval_4	26	0.00 ± 0.00	0.00 ± 0.00	0.59 ± 0.03	0.75 ± 0.10	1.00 ± 0.00	1.00 ± 0.00
yeast_me2	28	0.00 ± 0.00	0.00 ± 0.00	0.51 ± 0.04	0.57 ± 0.09	1.00 ± 0.00	1.00 ± 0.00
mammography	42	0.01 ± 0.02	0.00 ± 0.00	0.54 ± 0.03	0.56 ± 0.04	1.00 ± 0.01	1.00 ± 0.00
abalone_19	130	0.00 ± 0.00	0.00 ± 0.00	0.58 ± 0.05	0.80 ± 0.12	0.99 ± 0.02	1.00 ± 0.00
average		0.01 ± 0.01	0.00 ± 0.00	0.58 ± 0.03	0.68 ± 0.07	1.00 ± 0.00	1.00 ± 0.00

Table 3: Privacy attacks vs. augmented data.

Dataset	r	Naive metrics		MIA (AUC)	ReconSMOTE	
		(Accuracy)	(Precision)		(Precision)	(Recall)
ecoli	8.6	0.19 ± 0.15	0.93 ± 0.05	1.00 ± 0.00	0.43 ± 0.02	
abalone	9.7	0.21 ± 0.17	0.65 ± 0.07	1.00 ± 0.00	0.62 ± 0.01	
car_eval_34	12	0.00 ± 0.00	0.97 ± 0.01	1.00 ± 0.00	0.83 ± 0.03	
solarflare_m0	19	0.03 ± 0.06	1.00 ± 0.00	1.00 ± 0.00	0.95 ± 0.02	
car_eval_4	26	0.01 ± 0.04	1.00 ± 0.00	1.00 ± 0.00	1.00 ± 0.00	
yeast_me2	28	0.20 ± 0.12	0.99 ± 0.01	1.00 ± 0.00	1.00 ± 0.00	
mammography	42	0.25 ± 0.15	0.91 ± 0.04	1.00 ± 0.00	1.00 ± 0.00	
abalone_19	130	0.37 ± 0.14	1.00 ± 0.00	1.00 ± 0.00	1.00 ± 0.00	
average		0.16 ± 0.10	0.93 ± 0.02	1.00 ± 0.00	0.85 ± 0.01	

Table 4: Privacy attacks vs. synthetic data.

average AUC increases by 17% (comparing the third and fourth columns in Table 3). Larger imbalance further amplifies this effect. While similar intuitions have been noted previously [52], they were not supported by empirical evidence.

DistinSMOTE. Finally, we run DistinSMOTE on 25 SMOTE generations and report average precision/recall (two rightmost columns in Table 3). As expected from our analysis, we achieve perfect results across all datasets and imbalance levels. This shows that merely knowing SMOTE was used for augmentation is enough for an adversary to perfectly identify real records with minimal effort.

5.2 Synthetic Data

Next, we evaluate all attacks on synthetic data; see Table 4.

Naive Metrics. A widely used approach for evaluating privacy in synthetic data is the Distance to Closest Record (DCR) [61], which measures the average distance between synthetic and real records. DCR has been commonly applied to SMOTE and modern diffusion models [34, 42, 47, 59], but its interpretation is limited – an average distance alone provides little insight into privacy risks. To address this, we use a linkability attack [22], which builds on DCR and reports the accuracy with which an adversary could link two partial feature sets of a real record using synthetic data. For each dataset, we train 5 SMOTE models and evaluate linkability 5 times with varying feature subsets.

The results are unstable (see the leftmost column in Table 4): scores differ from zero only for low-dimensional settings ($d \leq 10$), while higher-dimensional datasets yield large variances that render DCR unreliable. This is expected, as DCR treats all features equally and is known to be an inadequate privacy measure [4, 19, 57].

MIA. We evaluate MIAs on synthetic data using the repeated classification game (similar to Section 5.1). We rely on the GroundHog attack [56], one of the most popular MIAs for synthetic tabular data. GroundHog extracts statistical features from generated datasets – such as column-wise minimum, mean, median, maximum, and pairwise correlations – and uses them to train a meta-classifier, which is then applied to unlabeled real and synthetic feature sets. To generate training features, we train 400 SMOTE models for in/out training features and another 200 SMOTE models for in/out testing features. Repeating this for 100 targets yields about 60k models per dataset.

As shown in Table 4 (second column), this results in substantial privacy leakage: AUC exceeds 0.9 in all but one dataset. The exception is abalone, which has the second-lowest imbalance ratio and the second-largest number of records, potentially leading to lower sensitivity. When imbalance increases (abalone_19), the MIA AUC rises to 1. Overall, these results demonstrate that SMOTE-generated data is highly susceptible to MIAs, even beyond trivial cases where data domain characteristics mainly drive leakage [20, 21].

ReconSMOTE. Next, we apply ReconSMOTE on 25 SMOTE generations per dataset, reporting average precision/recall (last two columns in Table 4). The attack achieves perfect precision on all datasets, which, as motivated in Section 4, is the most critical metric for reconstruction. Recall is also very high (see Figure 2), with an average of 0.85. It increases quickly with class imbalance, reaching 1 when $r \geq 20$. The recall values (per dataset) are in line with the expected approximate/exact bounds predicted by Theorem 3 and 4.

To further validate the expected bounds at finer granularity, we vary the imbalance ratio $\{5, 10, 20, 25, 50, 75, 100\}$ across all datasets and plot the average performance in Figure 3. As expected, recall increases exponentially with r (for fixed k), reaching 1 around imbalance 20. Overall, these findings highlight the risks of relying on SMOTE for synthetic data generation: in realistic settings, an adversary can reconstruct all real records with perfect confidence.

5.3 Take-Aways

We show that MIAs achieve high AUC across numerous targets vs. SMOTE: 0.68 against classifiers trained on augmented data and 0.93 against synthetic data. Moreover, the sensitivity of minority records increases by an average of 17% when classifiers are trained on augmented rather than original training data. Finally, our attacks, DistinSMOTE and ReconSMOTE, are able to i) distinguish real minority records from synthetic ones in augmented data, and ii) reconstruct real minority records from synthetic data with minimal assumptions and near-perfect accuracy.

6 Conclusion

Our work highlights the fundamental privacy limitations of SMOTE [7], one of the most widely adopted techniques for improved learning on imbalanced data. The effectiveness of our novel, near assumption-free attacks (DistinSMOTE and ReconSMOTE), demonstrates that real minority records – precisely the ones SMOTE aims to better represent – are exposed to significant privacy risk. Nonetheless, SMOTE remains an effective and easy-to-use technique in non-privacy-sensitive applications where utility is the primary concern. We are confident our findings will be valuable to researchers and practitioners deploying solutions that process or release sensitive data, and will motivate them to adopt more robust privacy-preserving techniques.

Limitations and Future Work. Our attacks currently operate on continuous data and are tested only on the original SMOTE implementation. However, our findings generalize to many SMOTE variants – such as BorderlineSMOTE [25], ADASYN [27], SVMSMOTE [44], and cluster/hybrid-based methods, etc. – as they all rely on line-segment interpolation to generate synthetic samples. Extending our attacks and defenses to these variants is a promising direction for future work.

Privacy-preserving variants of SMOTE have also been proposed under the framework of Differential Privacy [14, 15], including DP-SMOTE [38], which adds noise when estimating point distributions/nearest neighbors, and SMOTE-DP [62], which combines SMOTE with a DP generative model. However, SMOTE-DP largely ignores SMOTE’s increased sensitivity of minority records [36, 38, 52], a gap we confirm empirically

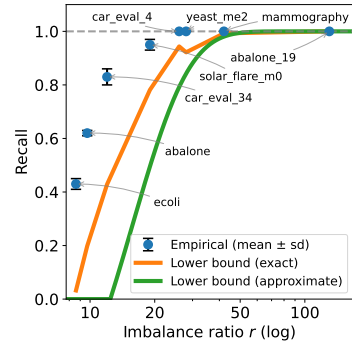


Figure 2: ReconSMOTE recall and lower bounds (per dataset).

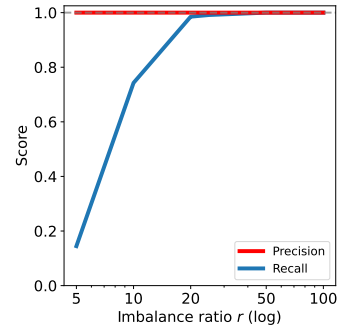


Figure 3: ReconSMOTE performance w/ varying r (all datasets).

(see Section 5.1). As none of these approaches provides open-source implementations, we leave evaluating their effectiveness to future work.

Ethics Statement. Our work does not involve attacking live systems or private datasets. Our goal is to demonstrate the importance of emphasizing privacy considerations and relying on established notions of privacy when processing sensitive, imbalanced data in critical domains.

References

- [1] ADR Wales. Scoping and Evaluation of Synthetic Data to Enhance Access to Data. <https://adrwales.org/wp-content/uploads/2025/04/BOLD-synthetic-data.pdf>, 2025.
- [2] Manal Alghamdi, Mouaz Al-Mallah, Steven Keteyian, Clinton Brawner, Jonathan Ehrman, and Sherif Sakr. Predicting Diabetes Mellitus using SMOTE and Ensemble Machine Learning Approach: The Henry Ford Exercise Testing (FIT) Project. *PloS ONE*, 2017.
- [3] Meenatchi Sundaram Muthu Selva Annamalai, Andrea Gadotti, and Luc Rocher. A Linear Reconstruction Approach for Attribute Inference Attacks against Synthetic Data. In *USENIX Security*, 2024.
- [4] Meenatchi Sundaram Muthu Selva Annamalai, Georgi Ganев, and Emiliano De Cristofaro. “What do you want from theory alone?” Experimenting with Tight Auditing of Differentially Private Synthetic Data Generation. In *USENIX Security*, 2024.
- [5] AWS. Transform Data. <https://docs.aws.amazon.com/sagemaker/latest/dg/data-wrangler-transform.html>, 2025.
- [6] Nicholas Carlini, Steve Chien, Milad Nasr, Shuang Song, Andreas Terzis, and Florian Tramer. Membership Inference Attacks from First Principles. In *IEEE S&P*, 2022.
- [7] Nitesh V Chawla, Kevin W Bowyer, Lawrence O Hall, and W Philip Kegelmeyer. SMOTE: Synthetic Minority Over-sampling Technique. *JAIR*, 2002.
- [8] Dingfan Chen, Ning Yu, Yang Zhang, and Mario Fritz. GAN-Leaks: A Taxonomy of Membership Inference Attacks against Generative Models. In *ACM CCS*, 2020.
- [9] Wuxing Chen, Kaixiang Yang, Zhiwen Yu, Yifan Shi, and CL Philip Chen. A Survey on Imbalanced Learning: Latest Research, Applications and Future Directions. *Artif. Intell. Rev.*, 2024.
- [10] DataCebo. SDMetrics. <https://docs.sdv.dev/sdmetrics/>, 2025.
- [11] Travis Dick, Cynthia Dwork, Michael Kearns, Terrance Liu, Aaron Roth, Giuseppe Vietri, et al. Confidence-Ranked Reconstruction of Census Microdata from Published Statistics. *PNAS*, 2023.
- [12] Zejin Ding. *Diversified Ensemble Classifiers for Highly Imbalanced Data Learning and Their Application in Bioinformatics*. PhD thesis, Georgia State University, 2011.
- [13] Irit Dinur and Kobbi Nissim. Revealing Information while Preserving Privacy. In *PODS*, 2003.
- [14] Cynthia Dwork, Frank McSherry, Kobbi Nissim, and Adam Smith. Calibrating Noise to Sensitivity in Private Data Analysis. In *TCC*, 2006.
- [15] Cynthia Dwork, Aaron Roth, et al. The Algorithmic Foundations of Differential Privacy. *Foundations and Trends in Theoretical Computer Science*, 2014.
- [16] Khaled El Emam, Lucy Mosquera, Xi Fang, and Alaa El-Hussuna. Utility Metrics for Evaluating Synthetic Health Data Generation Methods: Validation Study. *JMIR Med. Inform.*, 2022.
- [17] Hosam El-Sofany, Belgacem Bouallegue, and Yasser M Abd El-Latif. A Proposed Technique for Predicting Heart Disease Using Machine Learning Algorithms and an Explainable AI Method. *Sci. Rep.*, 2024.
- [18] Sara Fotouhi, Shahrokh Asadi, and Michael W Kattan. A Comprehensive Data Level Analysis for Cancer Diagnosis on Imbalanced Data. *J. Biomed. Inform.*, 2019.
- [19] Georgi Ganev and Emiliano De Cristofaro. The Inadequacy of Similarity-Based Privacy Metrics: Privacy Attacks Against “Truly Anonymous” Synthetic Datasets. In *IEEE S&P*, 2025.
- [20] Georgi Ganev, Meenatchi Sundaram Muthu Selva Annamalai, Sofiane Mahiou, and Emiliano De Cristofaro. The Importance of Being Discrete: Measuring the Impact of Discretization in End-to-End Differentially Private Synthetic Data. In *ACM CCS*, 2025.

[21] Georgi Ganев, Meenatchi Sundaram Muthu Selva Annamalai, Sofiane Mahiou, and Emiliano De Cristofaro. Understanding the Impact of Data Domain Extraction on Synthetic Data Privacy. In *ICLR SynthData*, 2025.

[22] Matteo Giomi, Franziska Boenisch, Christoph Wehmeyer, and Borbála Tasnádi. A Unified Framework for Quantifying Privacy Risk in Synthetic Data. *PoPETS*, 2022.

[23] Google Cloud. Learn about dataset transformations – Understand preprocessing, balancing, stratification, and dataset suitability for machine learning. https://cloud.google.com/vertex-ai/generative-ai/docs/prompt-gallery/samples/code_learn_about_dataset_transformations, 2025.

[24] Florent Guépin, Nataša Krčo, Matthieu Meeus, and Yves-Alexandre de Montjoye. Lost in the Averages: A New Specific Setup to Evaluate Membership Inference Attacks Against Machine Learning Models. *arXiv:2405.15423*, 2024.

[25] Hui Han, Wen-Yuan Wang, and Bing-Huan Mao. Borderline-SMOTE: A New Over-Sampling Method in Imbalanced Data Sets Learning. In *ICIC*, 2005.

[26] Haibo He and Edwardo A Garcia. Learning from Imbalanced Data. *IEEE TKDE*, 2009.

[27] Haibo He, Yang Bai, Edwardo A. Garcia, and Shutao Li. ADASYN: Adaptive Synthetic Sampling Approach for Imbalanced Learning. In *IJCNN*, 2008.

[28] Florimond Houssiau, James Jordon, Samuel N Cohen, Owen Daniel, Andrew Elliott, James Geddes, et al. TAPAS: A Toolbox for Adversarial Privacy Auditing of Synthetic Data. In *NeurIPS SyntheticData4ML*, 2022.

[29] ICO. Chapter 5: privacy-enhancing technologies (PETs). <https://ico.org.uk/media/about-the-ico/consultations/4021464/chapter-5-anonymisation-pets.pdf>, 2022.

[30] Bayrem Kaabachi, Jérémie Despraz, Thierry Meurers, Karen Otte, Mehmed Halilovic, Bogdan Kulynych, et al. A Scoping Review of Privacy and Utility Metrics in Medical Synthetic Data. *NPJ Digit. Med.*, 2025.

[31] Abdul Rehman Khalid, Nsikak Owoh, Omair Uthmani, Moses Ashawa, Jude Osamor, and John Adejoh. Enhancing Credit Card Fraud Detection: An Ensemble Machine Learning Approach. *BDCC*, 2024.

[32] G Charbel N Kindji, Lina Maria Rojas-Barahona, Elisa Fromont, and Tanguy Urvoy. Under the Hood of Tabular Data Generation Models: Benchmarks with Extensive Tuning. *arXiv:2406.12945*, 2024.

[33] Tanapol Kosolwattana, Chenang Liu, Renjie Hu, Shizhong Han, Hua Chen, and Ying Lin. A Self-inspected Adaptive SMOTE Algorithm (SASMOTE) for Highly Imbalanced Data Classification in Healthcare. *BioData Min.*, 2023.

[34] Akim Kotelnikov, Dmitry Baranchuk, Ivan Rubachev, and Artem Babenko. TabDDPM: Modelling Tabular Data with Diffusion Models. In *ICML*, 2023.

[35] Bogdan Kulynych, Mohammad Yaghini, Giovanni Cherubin, Michael Veale, and Carmela Troncoso. Disparate Vulnerability to Membership Inference Attacks. *PoPETS*, 2022.

[36] Ashly Lau and Jonathan Passerat-Palmbach. Statistical Privacy Guarantees of Machine Learning Preprocessing Techniques. In *TPDP*, 2021.

[37] Guillaume Lemaitre, Fernando Nogueira, and Christos K Aridas. Imbalanced-learn: A Python Toolbox to Tackle the Curse of Imbalanced Datasets in Machine Learning. *JMLR*, 2017.

[38] Yuliia Lut. *Privacy-Aware Data Analysis: Recent Developments for Statistics and Machine Learning*. PhD thesis, Columbia University, 2022. Chapter 3: Private Tools for Imbalanced Learning.

[39] Dionysis Manouskas and Sergül Aydöre. On the Usefulness of Synthetic Tabular Data Generation. In *ICML DMLR*, 2023.

[40] Microsoft. SMOTE. <https://learn.microsoft.com/en-us/azure/machine-learning/component-reference/smote>, 2024.

[41] Microsoft. Example pipelines & datasets for Azure Machine Learning designer. <https://learn.microsoft.com/en-us/azure/machine-learning/samples-designer>, 2025.

[42] Markus Mueller, Kathrin Gruber, and Dennis Fok. Continuous Diffusion for Mixed-Type Tabular Data. In *ICLR*, 2025.

[43] Mirza Muntasir Nishat, Fahim Faisal, Ishrak Jahan Ratul, Abdullah Al-Monsur, Abrar Mohammad Ar-Rafi, Sarker Mohammad Nasrullah, et al. A Comprehensive Investigation of the Performances of Different Machine Learning Classifiers with SMOTE-ENN Oversampling Technique and Hyperparameter Optimization for Imbalanced Heart Failure Dataset. *Sci. Program.*, 2022.

[44] Hien M. Nguyen, Eric W. Cooper, and Katsuari Kamei. Borderline Over-sampling for Imbalanced Data Classification. *IJKESDP*, 2009.

[45] ONS. Synthetic Data for Public Good. <https://datasciencecampus.ons.gov.uk/projects/synthetic-data-for-public-good/>, 2019.

[46] Shimaa Ouf, Kholoud T Mahmoud, and Manal A Abdel-Fattah. A Proposed Hybrid Framework to Improve the Accuracy of Customer Churn Prediction in Telecom Industry. *J. Big Data*, 2024.

[47] Wei Pang, Masoumeh Shafieinejad, Lucy Liu, Stephanie Hazlewood, and Xi He. ClavaDDPM: Multi-relational Data Synthesis with Cluster-guided Diffusion Models. In *NeurIPS*, 2024.

[48] Fabian Pedregosa, Gaël Varoquaux, Alexandre Gramfort, Vincent Michel, Bertrand Thirion, Olivier Grisel, et al. Scikit-learn: Machine Learning in Python. *JMLR*, 2011.

[49] Ke Peng, Yan Peng, and Wenguang Li. Research on Customer Churn Prediction and Model Interpretability Analysis. *PloS ONE*, 2023.

[50] Zhaozhi Qian, Rob Davis, and Mihaela van der Schaar. Synthcity: A Benchmark Framework for Diverse Use Cases of Tabular Synthetic Data. In *NeurIPS Datasets and Benchmarks Track*, 2023.

[51] Azra Ramezankhani, Omid Pournik, Jamal Shahrabi, Fereidoun Azizi, Farzad Hadaegh, and Davood Khalili. The Impact of Oversampling with SMOTE on the Performance of 3 Classifiers in Prediction of Type 2 Diabetes. *MDM*, 2016.

[52] Lucas Rosenblatt, Yuliia Lut, Eitan Turok, Marco Avella-Medina, and Rachel Cummings. Differential Privacy Under Class Imbalance: Methods and Empirical Insights. In *ICML*, 2025.

[53] Reza Shokri, Marco Stronati, Congzheng Song, and Vitaly Shmatikov. Membership Inference Attacks against Machine Learning Models. In *IEEE S&P*, 2017.

[54] Andrey Sidorenko and Paul Tiwald. Privacy-Preserving Tabular Synthetic Data Generation Using TabularARGN. *arXiv:2508.06647*, 2025.

[55] Joshua Snode, Gillian M Raab, Beata Nowok, Chris Dibben, and Aleksandra Slavkovic. General and Specific Utility Measures for Synthetic Data. *JRSSA*, 2018.

[56] Theresa Stadler, Bristena Oprisanu, and Carmela Troncoso. Synthetic Data – Anonymisation Groundhog Day. In *USENIX Security*, 2022.

[57] Zexi Yao, Nataša Krčo, Georgi Ganev, and Yves-Alexandre de Montjoye. The DCR Delusion: Measuring the Privacy Risk of Synthetic Data. In *ESORICS*, 2025.

[58] Jiayuan Ye, Anastasia Borovykh, Soufiane Hayou, and Reza Shokri. Leave-one-out Distinguishability in Machine Learning. In *ICLR*, 2024.

[59] Hengrui Zhang, Jian Zhang, Balasubramaniam Srinivasan, Zhengyuan Shen, Xiao Qin, Christos Faloutsos, et al. Mixed-Type Tabular Data Synthesis with Score-based Diffusion in Latent Space. In *ICLR*, 2024.

[60] Zhihong Zhao and Tongyuan Bai. Financial Fraud Detection and Prediction in Listed Companies Using SMOTE and Machine Learning Algorithms. *Entropy*, 2022.

[61] Zilong Zhao, Aditya Kunar, Robert Birke, and Lydia Y Chen. CTAB-GAN: Effective Table Data Synthesizing. In *ACML*, 2021.

[62] Yan Zhou, Bradley Malin, and Murat Kantarcioglu. SMOTE-DP: Improving Privacy-Utility Tradeoff with Synthetic Data. *arXiv:2506.01907*, 2025.

A Tighter Lower Bound on ReconSMOTE Recall

In this section, we derive a tighter lower bound on the recall of ReconSMOTE by relaxing two of the assumptions in Section 4.3, namely the Poisson approximation and the one-directional counting of C_{ij} . Specifically, we use the exact Binomial distributions and count C_{ij} in both directions to obtain more accurate values.

Recall that at each step of the SMOTE algorithm, we choose an $x_i \in X_{real}^1$ uniformly at random and then independently select one of its k nearest neighbors uniformly at random. To capture this structure, we represent the minority data by a KNN graph $G = (X_{real}^1, E)$, where edges E represent the neighboring relations among the minority samples. As before, we use $N(x_i)$ to denote the k nearest points to x_i from the minority set. For each $x_i \in X_{real}^1$, we add an edge $E_{i \rightarrow j}$ whenever $x_j \in N(x_i)$. Each synthetic data generated by SMOTE is associated with exactly one edge. Let α denote the probability that a nearest-neighbor relation is *mutual*; i.e., the probability that if $x_j \in N(x_i)$ then also $x_i \in N(x_j)$. In this case, a synthetic point lies on $E_{i \rightarrow j}$ if it

was generated along $E_{i \rightarrow j}$ or along $E_{j \rightarrow i}$. If $\alpha = 1$, then all nearest-neighbor edges are mutual, and $\alpha = 0$ corresponds to a completely one-sided nearest-neighbor graph, for which we usually refer to those edges as *exclusive*.

Recall that an edge is *reconstructed* if at least three synthetic records lie on its segment, and a real x_i is *identifiable* if there exist three reconstructed edges incident to x_i . For generating each synthetic point, we independently select an x_i with probability $1/n_1$ and then a neighbor $x_j \in N(x_i)$ with probability $1/k$. We denote the number of synthetic data points generated between x_i and x_j by C_{ij} . Let $B_{ij} := \mathbb{I}\{x_i \in N(x_j)\}$ and $x_j \in N(x_i)\}$ (*mutuality indicator*) with $\Pr\{B_{ij} = 1\} = \alpha$. Then

$$C_{ij} \mid B_{ij} = 0 \sim \text{Binom}\left(n_0 - n_1, \frac{1}{n_1 k}\right), \quad C_{ij} \mid B_{ij} = 1 \sim \text{Binom}\left(n_0 - n_1, \frac{2}{n_1 k}\right).$$

Assumption 4 (Local non-degeneracy). *For any $x_i \in X_{\text{real}}^1$, all edges $\{E_{i \rightarrow j} : x_j \in N(x_i)\}$ have pairwise distinct directions.*

Under Assumption 4, the intersection of any three reconstructed edges incident to x_i uniquely identifies x_i .

Lemma 1 (Reconstructed edge probability). *For any edge of G ,*

$$\Pr\{C_{ij} \geq 3\} = (1 - \alpha) \Pr\{\text{Binom}(n_0 - n_1, \frac{1}{n_1 k}) \geq 3\} + \alpha \Pr\{\text{Binom}(n_0 - n_1, \frac{2}{n_1 k}) \geq 3\} =: p_{\text{edge}}(\alpha).$$

Proof. Condition on B_{ij} and compute the average. If $B_{ij} = 0$, then only one direction contributes to the count; if $B_{ij} = 1$, both directions do. \square

Lemma 2 (Lower-bound on per-node identifiability). *Fix $x_i \in X_{\text{real}}^1$ and its k outgoing directed edges $\{E_{i \rightarrow j} : x_j \in N(x_i)\}$. Then, we have*

$$\Pr\{x_i \text{ identifiable}\} \geq \max\left\{0, \frac{k p_{\text{edge}}(\alpha) - 2}{k - 2}\right\} =: L_{id}, \quad (2)$$

and this lower bound is tight.

Proof. Declare an edge reconstructed if $C_{ij} \geq 3$ and set $E_{i \rightarrow j}^{\text{rec}} := \mathbb{I}\{C_{ij} \geq 3\}$. Let $S_i = \sum_{j=1}^k E_{i \rightarrow j}^{\text{rec}}$. From Lemma 1, each edge has marginal $\Pr\{E_{i \rightarrow j}^{\text{rec}} = 1\} = p_{\text{edge}}(\alpha)$, so $\mathbb{E}[S_i] = k p_{\text{edge}}(\alpha)$. Then, we have

$$\begin{aligned} \mathbb{E}[S_i] &= \mathbb{E}[S_i \mathbb{I}\{S_i \leq 2\}] + \mathbb{E}[S_i \mathbb{I}\{S_i \geq 3\}] \\ &\leq \mathbb{E}[2 \mathbb{I}\{S_i \leq 2\}] + \mathbb{E}[k \mathbb{I}\{S_i \geq 3\}] \quad (\text{since } S_i \leq k \text{ a.s.}) \\ &= 2 \Pr\{S_i \leq 2\} + k \Pr\{S_i \geq 3\}. \end{aligned}$$

Since $\Pr\{S_i \leq 2\} = 1 - \Pr\{S_i \geq 3\}$, we obtain

$$\mathbb{E}[S_i] \leq 2 + (k - 2) \Pr\{S_i \geq 3\},$$

hence

$$\Pr\{S_i \geq 3\} \geq \frac{\mathbb{E}[S_i] - 2}{k - 2} = \frac{k p_{\text{edge}}(\alpha) - 2}{k - 2}.$$

Truncating at 0 accommodates the trivial case $k p_{\text{edge}}(\alpha) \leq 2$.

Moreover, the bound cannot be improved using only the edge-wise success probabilities. Consider constructing $(E_{i \rightarrow j}^{\text{rec}})_{j=1}^k$ so that $S_i = \sum_{j=1}^k E_{i \rightarrow j}^{\text{rec}}$ takes values only in $\{2, k\}$. Choose the mixture weights so that $\mathbb{E}[S_i] = k p_{\text{edge}}(\alpha)$. In this case, the inequality holds with equality, meaning that the lower bound is tight. \square

Theorem 4 (ReconSMOTE expected recall (exact)). *We have*

$$\mathbb{E}[\text{Recall}] := \mathbb{E}\left[\frac{1}{n_1} \#\{x_i \in X_{\text{real}}^1 : x_i \text{ identifiable}\}\right] \geq L_{id}, \quad (3)$$

where L_{id} is defined in Equation 2.

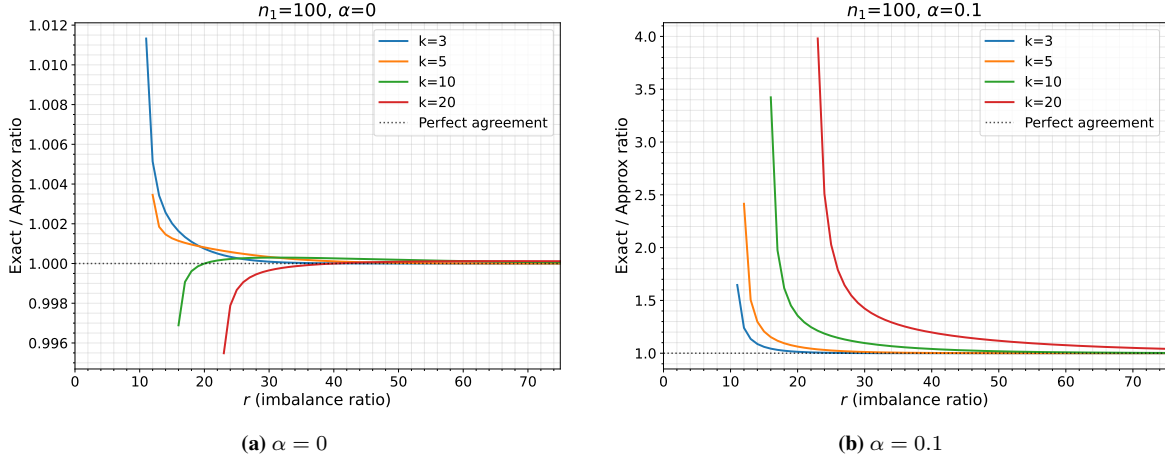


Figure 4: Exact/approximate bound ratios for two levels of mutuality.

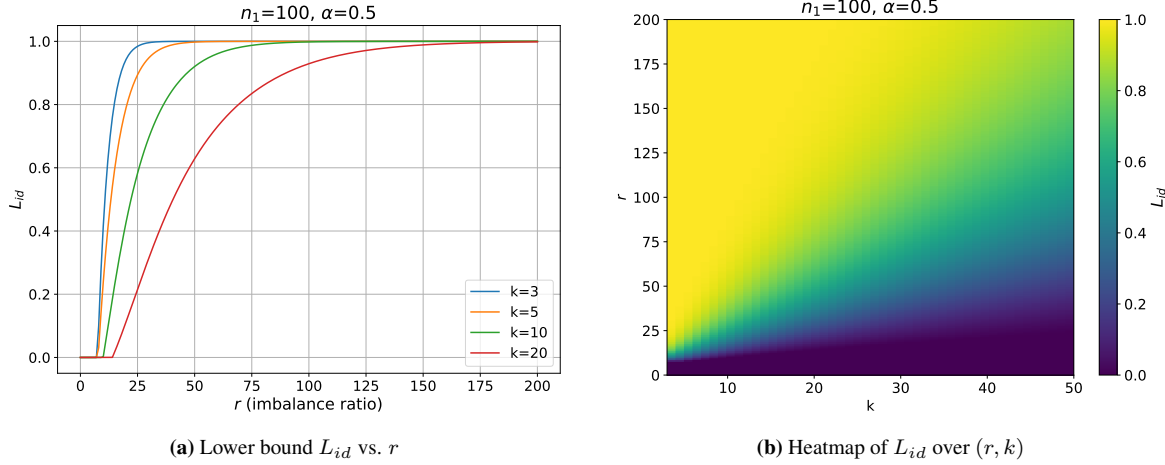


Figure 5: Comparison of two visualizations of the exact bound.

Proof. By Lemma 2, we have $\Pr\{x_i \text{ identifiable}\} \geq L_{id}$ for every i , so

$$\mathbb{E}[\text{Recall}] = \frac{1}{n_1} \sum_{i=1}^{n_1} \Pr\{x_i \text{ identifiable}\} \geq L_{id}.$$

□

B Lower Bounds of ReconSMOTE Recall Visualizations

To complement the theoretical results in Section 4.3 (approximate bound, A_{id}) and Appendix A (exact bound, L_{id}), we visualize the bounds under different conditions.

We start by showing the ratio between the exact bound and the approximate bound as a function of the imbalance ratio r in Figure 4. When $\alpha = 0$ (Figure 4a), the approximate bound closely matches the exact one for all k , especially for larger imbalance ratio. In contrast, even a small amount of mutuality ($\alpha = 0.1$; Figure 4b) introduces a noticeable deviation of the lower bound.

Next, in Figure 5, we focus on the exact bound L_{id} under varying imbalance ratios r and neighborhood sizes k (with $n_1 = 100$ and $\alpha = 0.5$ fixed). Figure 5a shows that L_{id} steadily increases as the oversampling ratio r rises. For small k , even a moderate oversampling ratio results in significant identifiability. However, for larger k , a higher oversampling ratio is required. The heatmap in Figure 5b clearly illustrates this interaction.

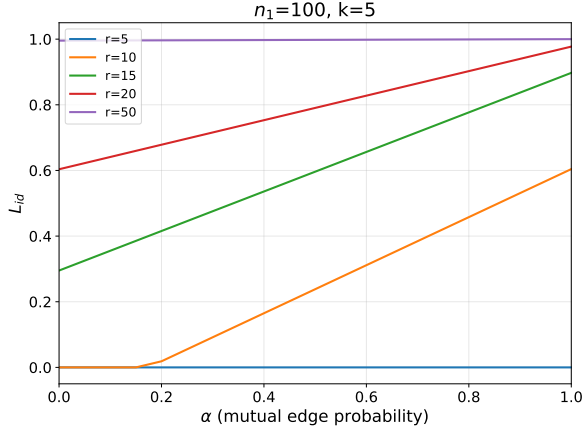


Figure 6: Exact bound as a function of α for different imbalance ratios r .

In the upper-left area, where k is small and r is large, L_{id} quickly approaches 1. This indicates almost perfect identifiability. In contrast, in the lower-right area, where k is large and r is small, L_{id} is close to zero. This suggests that the reconstructed edges are not dense enough to reach high identifiability. Overall, these plots confirm the trade-off: identifiability improves with oversampling, but its efficiency depends strongly on the neighborhood parameter k .

Finally, Figure 6 presents the exact bound L_{id} as a function of α for several imbalance ratios r . The curves illustrate the sensitivity of L_{id} to the graph structure. For example, when $r = 10$, small increases in α would lead to substantial changes in L_{id} , highlighting how mutuality in the KNN graph strongly influences privacy leakage.